Indonesian Journal of Electrical Engineering and Informatics (IJEEI)
Vol. 12, No. 4, December 2024, pp. 858~869
ISSN: 2089-3272, DOI: 10.52549/ijeei.v12i4.5885

Artificial Intelligence-Based DS-PSO Algorithm for Enhanced Frequency Response in Digital IIR Filters

Wijdan Rashid Abdulhussien[1], Jehan Kadhim Shareef Al-Safi[2], Wasan M. Jwaid [3]

[1]Information Technology Department, Computer Science and Mathematics College.
[2]Department of Digital Media, Faculty of Media.
[3]Department of Banking and Finance, Faculty of Administration and Economics.
[1, 2, 3] University of Thi-Qar, Thi-Qar, Iraq.

Article Info

Article history:
Received Sep 14, 2024
Revised Nov 7, 2024
Accepted Nov 17, 2024

Keywords:
AI
Digital Filter
Filter Design
Infinite Impulse Response
Optimization Algorithms

ABSTRACT

Digital elliptic filters, as a type of infinite impulse response (IIR) digital filter, play a crucial role in signal processing applications. Despite their widespread use, there remains a significant research gap in optimizing their frequency response to better approximate desired magnitude responses. This study addresses this gap by introducing an innovative optimization technique that leverages the DS-PSO (Dynamic & Static-Particle Swarm Optimization) algorithm. Based on artificial intelligence, the DS-PSO method uniquely integrates topologies (dynamic and static) into particle swarm optimization (PSO), enabling more precise analysis of pole positions derived from a filter's transfer function coefficients. The primary research problem lies in approximating the frequency response of digital IIR elliptic filters to match a desired magnitude response. Traditional methods often fail to achieve this due to limitations in their optimization techniques. The proposed DS-PSO algorithm addresses this by setting a slightly more significant maximum pole radius (R*max*) than 1.0, surpassing the pre-established pole radius (R). This approach allows for a more accurate approximation of the frequency response. This feature distinguishes it from previous studies that employed genetic algorithms (GA) and semi-definite programming (SDP) techniques, which reported lower R*max* values. The results of this study demonstrate the effectiveness of the DS-PSO algorithm in improving the frequency response of digital IIR elliptic filters. The proposed method successfully approximates the desired magnitude response by designing 4th and 12th-order lowpass digital IIR elliptic filters while maintaining stability at a high average. This makes the technique particularly suitable for determining frequency response boundaries in electronics or communications systems. The contribution of this research extends beyond the immediate results. By introducing and validating the DS-PSO algorithm, this study provides a robust framework for future research in optimizing digital IIR filters. The findings not only enhance the design of digital elliptic filters but also open new avenues for improving other types of IIR filters and signal processing applications. This paper establishes a foundation for further research in signal processing and other fields, with significant theoretical and practical implications.

Corresponding Author:
Wijdan Rashid Abdulhussien,
Information Technology Department,
Computer Science and Mathematics College,
University of Thi-Qar, Thi-Qar, Iraq.
Email: wijdan_rashid@utq.edu.iq

1. INTRODUCTION

Digital filters are available in "finite impulse response" (FIR) and "infinite impulse response" (IIR), which are used for signal processing applications. These filters have filter transfer function coefficients; these coefficients must be taken in such a way as to obtain the optimally desired response for approximating frequency response when an IIR digital filter's design has been improved [1]. However, the optimal impulse response is doubled when digital filters are designed using the window functions method; these functions depend on the parameters necessary to design the filter, such as (Transition Band), (Passband Ripple), and (Stopband Ripple) [2]. Additionally, the Windows functions method provides no adequate control over frequency response and other filter parameters, like transmission band. Therefore, the IIR range of the optimal filter in the specified window function must be hidden when the actual response has been designed with those window functions [3]. However, the stability condition of the digital filter must be achieved when optimizing filter design [4].

Omoifo OI et al. [1] transformed the finite stability position via the variable transformation into the whole coefficient space; constrained design problems are liberated in the newly created space. Though transformation increases objective function nonlinearity, locating precise, global optimum solutions makes it more difficult.

B. Limketkai et al. [2], suggested an approach of optimization-based synthesizing to formulate the limitations and specifications on the magnitude square function and the conditions of stability obtained through Rouche's theorem as the constraints of the semidefinite matrix. It then casts the problem of magnitude response approximation as the problem of semidefinite programming (SDP). X. Lai et al. [3] developed Digital IIR filters with magnitude- and phase-response specifications by solving sub-problems with accompanying phase responses, which converge with the solution for the problem of the original magnitude response approximation. Lai et al. utilized the Gauss-Newton (GN) technique and an elliptic-error constraint to address the challenge of simultaneously approximating the accurate magnitude and phase responses. The problem associated with the initial approximation of the magnitude-response can be resolved by continuously updating the phase response. Additionally, the problem has easily incorporated the pole radius (R) constraint into the problem [4]. The resultant digital filters had the value of the maximum pole radius (R_{max}) close to 1.0, and this value was smaller than the value which was predetermined for R, like in [4] and [2].

Intelligent optimization algorithms are computational techniques developed for efficient resolution of complex optimization problems [5]. Particle swarm optimization (PSO) is a well-known example of artificial intelligence (AI) techniques [6]. The PSO algorithm was developed by Kennedy and Eberhart in [7]. Compared to alternative methods, PSO is commonly utilized for addressing optimization problems due to its efficiency and simplicity.

The improvement of digital IIR filter by artificial intelligence based optimization algorithm has also been the subject of many contemporary investigations [8]–[14]. Furthermore, Dabas et al. were the ones who were the first to introduce the technology that made it possible for the digital IIR filter to be developed and improved via the use of the PSO algorithm [15]. Hammou et al. applied an improved version of PSO, called Cooperation-Hierarchization PSO (CHPSO), to IIR system identification [16]. Furthermore, the used method for developing eighth-order digital IIR filters was Dynamic & Static-Particle Swarm Optimisation (DS-PSO) [17]. The Artificial intelligence-based DS-PSO algorithm demonstrated superior performance compared to the the simulated annealing algorithm (SA), the genetic algorithm (GA), the fuzzy gravitational search algorithm (FGSA), with mean values of 70.40%, 57.80%, and 55.21%, respectively. Furthermore, the DS-PSO method aimed to optimize the passband, stopband, and transition band characteristics between the initial and target responses of the IIR filter. This optimization was achieved by using the non-linear mean square error (SE) metric. According to the study conducted by [18], it has been shown that digital IIR filters based on DS-PSO exhibit superior performance compared to MDI-PSO and DI-PSO digital IIR filters. The improvement in performance ranges from 10% to 90% for the DS-PSO over the MDI-PSO, and from 50% to 90% for the DS-PSO over the DI-PSO, as measured in terms of the SE.

In this research, to analyse the digital IIR elliptic filter's frequency response will be used optimisation method. This inquiry involves determining the necessary size of the response. This experiment used an approach that included static and dynamic topologies with the PSO methodology. The approach is called DS-PSO. According to [6], the DS-PSO shows great promise as an artificial intelligence (AI) classification tool.

Although the PSO technique is straightforward to apply and effective, it has a considerable challenge with premature convergence. Unlike the DS-PSO approach, this strategy promotes search space exploration by endowing the particles with many neighbours [19]. The proposed method's capacity to efficiently identify alternate topologies, namely dynamic and static neighbors for the transfer function coefficients of each digital IIR elliptic filter, enhances the optimization of the suggested filter's transfer function coefficients. This study aims to ascertain the ideal value of R_max for constructing an elliptic digital filter using the existing

methodology. The stability of the elliptic digital filter is, therefore, guaranteed. The objective of giving a simulated example is to demonstrate the approach's effectiveness and compare it with existing tactics.

This paper's structure is as follows: The next section discusses the digital IIR filter. Section 3 discusses the maximum pole radius for the digital IIR filter. Section 3 introduces the AI-based DS-PSO algorithm. The Section 5 of this paper presents the simulation experiments, obtained results, comparisons, and numerical analysis. Conclusions are drawn in Section 6.

2. DIGITAL IIR FILTER

The IIR digital filter types are Butterworth, Chebyshev, and elliptic. These digital filters have a recursive implementation of the IIR [20]. Also, these filters can minimize the transition band, obtaining a better frequency response of the same order; the error between outputs of an unknown digital IIR filter system will be minimized when setting the parameters of the digital IIR filter by using intelligent algorithms[21]. With the adaptive IIR system described in [16], and the proposed optimization algorithm in this paper, a block diagram is designed in Figure 1 for an IIR system identification process.

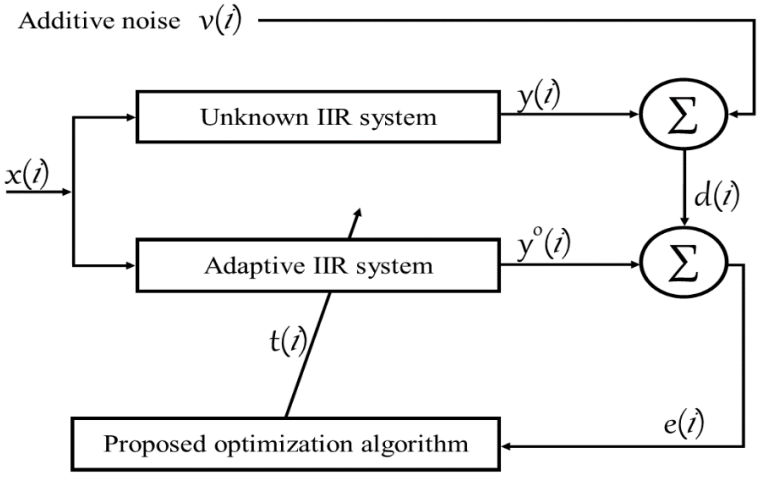

Figure 1. System identification block diagram utilizing IIR filter and used optimization algorithm.

Figure 1 $x(i)$ represents an unidentified IIR system's input, $y(i)$ represents an unidentified IIR system's output, $y^o(i)$ represent an adaptive IIR system's output, and $v(i)$ represents a noise signal applied to $y(i)$. Here, $d(i)$ denotes the output of an unidentified IIR system with noise, $e(i)$ denotes the generated error signal, and $t(i)$ denotes the input sample total number. The IIR digital filter's (input and output) relationship is shown in eq. (1).

$$y(i) + \sum_{k=1}^{n} a_k\, y(i-k) = \sum_{k=0}^{m} b_k x(i-k) \tag{1}$$

where $x(i)$ denotes the filter's input, $y(i)$ is the filter's output, and the n variable denotes the filter's order, and $m = n - 1$ assuming that $a_0 = 0$. A relationship exists between the stability criterion and the digital IIR filter transfer function. This is attributable to the function's presence of a denominator, as shown in equation (2) [22].

$$H(z) = \frac{\sum_{k=0}^{m} b_k z^{-k}}{1+\sum_{k=1}^{n} a_k z^{-k}} \tag{2}$$

$H(z)$ evaluating along the unit circle by $z = e^{j\omega}$. Thus, the frequency response is obtained as in eq. (3).

$$H(\omega) = \frac{\sum_{k=0}^{m} b_k e^{-jk\omega}}{\left(1+\sum_{k=1}^{n} a_k e^{-jk\omega}\right)} \tag{3}$$

Where, $\omega = [0, \pi]$, which is represented by digital frequency samples, $b = [b_1, b_2, \dots, b_k]$ and $a = [a_1, a_2, \dots, a_k]$ are coefficients vectors real-valued for the numerator and denominator of a filter, whereas the required frequency response is the magnitude (D_0) on a dense grid Ω_0 locates within the frequency interval$[0, \pi]$; this is shown in eq. (4).

$$E(\omega, g, a, b) = \left|H(e^{j\omega}, g, a, b)\right| - D(\omega) \tag{4}$$

Where g is the gain of the zero frequency; minimax estimation, as delineated in equation (5), may articulate the estimate of the error between the (actual and intended) magnitude responses.

$$\min_{g,a\epsilon S(\rho),b} \max_{\omega\epsilon\Omega} W(\omega)|E(\omega,g,a,b)| \tag{5}$$

where $W(\omega) > 0$ a function of weight, $S(\rho) = \{a\epsilon R^N |$ all zeros of $A(z,\ a)$ are centering within a circle of radius ρ centered at the origin$\}$, And $\Omega = \Omega_p \cup \Omega_s$ is a subset of Ω_0 with $\Omega_p \subset \Omega_0$ and $\Omega_s \subset \Omega_0$ denoting the passband and stopband frequency sets, respectively; this can be represented as in eq. (6).

$$\delta(\omega) = max_{\omega\epsilon\Omega} W(\omega)|E(\omega,g,a,b)| \tag{6}$$

where $\delta(\omega)$ signifies the weighted magnitude response error's upper-bound function on Ω; moreover, the minimax approximation problem can be described by equations (7 and 8) [3].

$$\min_{g,a\epsilon S(\rho),b,\delta(\omega)} ||\ \delta(\omega)||_\rho \tag{7}$$

$$W(\omega)|E(\omega,g,a,b)| \leq \delta(\omega), \omega\epsilon\Omega \tag{8}$$

3. THE VALUE OF MAXIMUM POLE RADIUS (R*max*) FOR IIR FILTER

The maximum pole radius (R_{max}) must be set to the best possible value when designing digital IIR filters; this is a precondition for resolving the issue of approximating the frequency response with desirable magnitude response. The solution to this problem is essential in achieving one of the conditions of stability for the Digital IIR filter .

For the stability of an IIR filter, all poles must show within the z-plane's unit circle. The inaccuracy in the approximation band tends to be concentrated in the transition band when applying the minimax criterion. Then, a magnitude ripple arises in a transition band, and poles tend to be close to the unit circle. (R_{max} can limit as shown in equations (9 and 10) [23]:

$$\varphi(R_{max}) = \{_0^{R^2_{max}} \quad ,\ _{,\text{Otherwise}}^{R_{max}} \geq r \tag{9}$$

$$R_{max} = max_{m=1,\dots,M}|R_m| \tag{10}$$

Usually, the value of the R_{max} is set to a value lesser than 1 to ensure that the filter coefficients stabilize following truncation because a truncation occurring for filter coefficients when designing the IIR digital filter can lead to pole shifts. Thus, after truncation, the filter's stability ensures if the digital filter has the value of the R_{max} close to 1.0.

As for the filter's transfer function in eq. (11), the coefficients found in the denominator are connected with the value of R_{max}, according to the case principle mentioned in [24],

$$H(z) = \frac{B(z)}{A(z)} = \frac{\sum_{i=0}^{M} b_i z^{-1}}{\sum_{i=0}^{N} a_i z^{-1}} \tag{11}$$

where $a_0 = 1, a_i$ with $i = 1,2 \dots N$ and b_i with $j = 0,1,2, \dots, M$ represent real coefficients. These coefficients are used in optimization as determination variables, such as $\delta_x = x_{(k+1)} - x_{(k)}$, where $x_{(k)} = [b_{0(k)}\ b_{1(k)} \dots\ b_{M(k)}\ a_{1(k)}\ a_{2(k)} \dots\ a_{N(k)}]^T$ for *kth* iteration, where *T* denotes the transpose operation. X_k may be substituted to produce $z = e^{j\omega}$ in $H(z)$, the equivalent frequency response $H(e^{j\omega})$, where ω denotes the frequency within radians per second (rad/s) [20].

According to the reasoning principle, the digital IIR filter's poles are all contained within a circle with a radius of R_{max} centered on the origin of the derivative of a denominator argument of a transfer function $\Phi(\omega, \mathrm{R.a})$ satisfies eq. (12) [25]:

$$[\tfrac{1}{\pi} \int_0^\pi \nabla_a \Phi(\omega,R,a) d\omega]^T\ a = 0 \tag{12}$$

where $\Phi(\omega,R,a) = \frac{d}{d\omega}\ argA(Re^{j\omega}),\ a = a_{k+1} - a_k$ and R is equal to R_{max}. The $Re^{j\omega}$ is obtained by substituting $z = Re^{j\omega}$ into the denominator of $H(z)$ in eq. (11).

4. THE ARTIFICIAL INTELLIGENCE-BASED DS-PSO ALGORITHM

An artificial intelligence (AI) approach is used in this paper, because of the potential of using intelligent AI-based optimization algorithms to address optimization problems [26]. Particle Swarm Optimization (PSO) and its variations, such as dynamic & static-particle swarm optimization (DS-PSO) (The Artificial intelligence-based DS-PSO algorithm), are notable examples of AI techniques. It is one of the hybrid PSO algorithms that

use both (dynamic & static) PSO (DS-PSO). The traditional PSO algorithm uses a search space to initialize the particle swarm. The swarm subset or neighborhood, velocity, and random position are assigned per particle to keep track of the swarm's particles. Each particle in an algorithm performs a functional evaluation at its present position at every iteration. The current position becomes the particle's new personal best (P_{best}). If the existing solution's fitness is higher than the particle's existing P_{best}. Eq. (13) and Eq.(15) are provided to update the (velocity and position) of the particle. The (DS-PSO and PSO) algorithms exhibit considerable similarities. This is due to DS-PSO integrating the topologies of both (dynamic & static) variants of traditional PSO.

The DS-PSO method assigns a distinct topology to each particle, differentiating between (dynamic & static) neighborhoods. This represents a crucial contrast between the two methodologies. This is the fundamental distinction. Conversely, the supplementary dynamic designs are not intended to facilitate early convergence; instead, they are designed to promote search space exploration. A random topology is also generated during the implementation of the algorithm. On the other hand, the static topology preserves the standard PSO's exploitative properties absent in other dynamic PSO algorithms.

The neighborhood bests (N_{Pbest}) of all the DS-PSO's topologies affect the particles, as swarm particles are updating their velocities (V) and positions (P) according to the equations (14 and 15).

$$V_p(i) = C_C[V_p(i-1) + C_1R_1\big(P_P(i-1) - X_P(i-1)\big) + C_2R_2\big(N_{Pbest}(i-1) - X_P(i-1)\big) \quad (13)$$

$$V_p(i) = C_C[V_p(i-1) + C_1R_1\big(P_P(i-1) - X_P(i-1)\big) + C_2R_2\big(D_{Pbest}(i-1) - X_P(i-1)\big) + C_3R_3\big(S_{Pbest}(i-1) - X_P(i-1)\big)\ ] \quad (14)$$

$$X_p(i) = X_P(i-1) + V_p(i) \quad (15)$$

The above equations $V_p(i)$represent the velocity and $X_p(i)$ represents the position of the particle p at iteration i. $P_P(i)$, $D_{Pbest}(i)$ and $S_{Pbest}(i)$ denote the particle p, personal, dynamic, and Static optimal solutions identified up to this point in iteration i.

The (C_C) is a constriction coefficient commonly set to around 0.7298438 to avoid exploding velocities. In eq. (13), C_1 and C_2 represent acceleration coefficients that increase particle p's attraction to P_P, and N_{Pbest}, respectively. Standard PSO has acceleration coefficients C_1 and C_2 of 2.05 per one and a total acceleration coefficient of 4.1. Additionally, C_1, C_2 and C_3 represent acceleration coefficients used in eq. (14) to increase particle p's attraction to $P_P(i)$, $D_{Pbest}(i)$ and $S_{Pbest}(i)$, respectively. Furthermore, because each particle has drawn to the optimum dynamic and static performance, it is also drawn to the optimum personal performance. Three acceleration coefficients are found for the DS-PSO algorithm instead of the standard PSO algorithm's two acceleration coefficients. These coefficients of acceleration are C_1, C_2 and C_3, which are set to 4.1/3.

To encourage exploration, per of the velocity equation position components is multiplied with the vector of R_1, R_2 and R_3 randomly generated values, which are in the range [0,1]. Each component of V_p must be kept within a $[V_{min}; V_{max}]$, range to keep particles contained within the search space, where $[V_{min}; V_{max}]$ is the search space's minimum and maximum values. Instead of being impacted by one neighborhood's best N_{Pbest}, particle p is prejudiced for D_{Pbest} and S_pbest within DS-PSO; therefore, this will be the best solution with the dynamic and static topologies of particles p, respectively [19], [27], [28]. Pseudocode flow of DS-PSO algorithm process sequence in [17]–[19]**.**

5. THE SIMULATION AND RESULTS

In the simulation process, a 4th-order lowpass digital IIR elliptic filter has been designed; this design has been done by the ellip () function used to design the digital IIR elliptic filter by MatLab programming. This function helps determine the values of the filter transfer function's coefficients. These coefficients are treated as particles within a swarm in the used DS-PSO algorithm to design and optimize the filter, where the filter coefficients are used in the optimization process.

The used algorithm determines the multiple topologies as dynamic and static neighborhoods for any of the designed filter's transfer function coefficients based on poles' positions. We could get the optimal filter transfer function coefficients with these dynamic and static neighborhoods. The best coefficients are used to formulate a magnitude response approximation problem. Thus, the desired response to the optimum approximate frequency response is obtained, and given that the desired response is achieved when the value of R_{max} value is close to 1.0, the value of R_{max} is calculated by applying the following equations (16, 17, and 18):

$$\omega = \kappa\pi/I \quad (16)$$

$$\tau = T/(1-R) \quad (17)$$

$$R_{max} = exp(-T/\tau) \quad (18)$$

The ω (Omega) is the velocity or angular frequency (measured in rad/s), k is the gain, I is the number of iterations, f is the ordinary frequency (measured in Hertz), T is the sampling interval in second or the period (measured by seconds), τ is the time of decay constant and R_{max} is the maximum pole radius. Also, the control parameters are taken after analysis for the algorithm system, as the control parameters are set for the DS-PSO algorithm by variables and values assigned to those variables in Table 1.

Table 1. The DS-PSO algorithm's control parameters.

Parameter	C_1	C_2	C_3	V_{max}	V_{min}	I_{max}	Ps
Values	4.1/3	4.1/3	4.1/3	2	-2	400	50

In Table 1, (C_1, C_2, and C_3) are the values of acceleration coefficients. These accelerations' coefficients are controlling in local and global search processes: the (V_{max}) is the maximum search space value, the (V_{min}) is the minimum search space value, the maximum iteration is referred to as I_{max}, and the population or swarm size in a search space is referred to as Ps.

Since the simulation attempts to solve the frequency response approximation problem by digital IIR elliptic filter with the desired magnitude response, the best R_{max} value must be obtained through this simulation when the value of the R_{max} is close to 1.0. However, the value of R should be predetermined when designing a digital IIR elliptic filter, as the predetermined value of the R must be not greater than 0.999. Results of previous studies for digital IIR elliptic filter design of the same type by SDP and GN in [2], [4]. This paper's simulation results will be compared to earlier research, as the parameters regulated for the digital IIR elliptic filter will come as in Table 2.

In Table 2, ellip () is a function, as mentioned at the beginning of this section, where the lowpass is typed from filters' types: lowpass, highpass, passband, and stopband. Also, the parameter of the passband (pb) is from the parameters necessary to design a filter that determines the filter's band-pass when designing the filter. Also, the parameter of the stopband (sb) is from the parameters necessary to design a filter, which determines the filter's band-stop when designing the filter. The h is the predetermined value of b while designing the IIR digital elliptic filter.

Table 2. The parameters for elliptic Digital IIR filter design.

Parameters	Model First/Values	Model Second/Values
Function	ellip( )	ellip()
Filter type	Lowpass	Lowpass
Passband (pb)	$[0,0.2\pi]$	$[0,0.5\ \pi]$
Stopband (sb)	$[0.45\ \pi, \pi]$	$[0.55\ \pi, \pi]$
Pole radius (R)	0.92 and 0.999	0.999
Filter order	4	12

After designing the required digital IIR elliptic filter by the proposed algorithm and calculating the value of R_{max}, a comparison was made between the value of R_{max} obtained by this simulation and that of R_{max} obtained from previous studies as shown in Tables 3, 4, and 5.

Table 3. Comparison of maximum pole radius values using different methods with 4th order and R= 0.92.

Ref.	[4]	[2]	In this paper
Method	SDP	GN	DS-PSO
Maximum pole radius values	0.9200	0.9173	0.9231

Table 4. Comparison of maximum pole radius values using different methods with 4th order and R= 0.999

Ref.	[4]	[2]	In this paper
Method	SDP	GN	DS-PSO
Maximum pole radius values	-	0.9423	0.99900049

Table 5. Comparison of maximum pole radius values using different methods with 12th order and R= 0.999

Ref.	[4]	[2]	In this paper
Method	SDP	GN	DS-PSO
Maximum pole radius values	-	0.9781	0.99900049

Tables 3, 4, and 5 represents the maximum pole radius values R_{max} calculated after designing the (elliptic) digital IIR filters, and the methodology used in the development of the (elliptic) digital IIR filter. This comparison is made between the results of the R_{max} obtained when (elliptic) digital IIR filter design by employing the DS-PSO algorithm in this simulation and other results of the R_{max} in previous studies, that are obtained when (elliptic) digital filter design by SDP and GN. Additionally, the following comparison is between three digital IIR filter design methods: (SDP, GN, and DS-PSO). Also, the R_{max} has different values with every method of these methods.

In Table 3, from (elliptic) digital IIR filter design by the predetermined value of R 0.92 with 4th-order of the filter, the R_{max} had values range from 0.9061 to 0.92 when using the SDP method, the value of R_{max} equal to 0.9173 when using the GN method, and the value of R_{max} equal to 0.9231 when using the DS-PSO algorithm. However, the R_{max}'s value is far less than or similar to the R's value when using the SDP method. Additionally, the R_{max}'s value is less than the R's value when the GN method is used, while the R_{max}'s value by employing the DS-PSO algorithm is more significant than the R's value.

In Tables 4, from the digital IIR elliptic filter design by the predetermined value of R 0.999 with the 4th-order of the filter. The R_{max} value is equal to 0.9422 and 0.9423 when using the GN method. The value of R_{max} equals 0.99900049 when using the DS-PSO algorithm. However, the value of R_{max} with the GN method is less than the R's value, while the R_{max}'s value by employing the DS-PSO algorithm is more significant than R's value.

In the Tables 5, from digital IIR elliptic filter design by the predetermined value of R 0.999 with 12th order of the filter, the value of R_{max} equal to 0.9781 when using the GN method, and the value of R_{max} equal to 0.99900049 when using the DS-PSO algorithm. However, the value of R_{max} with the GN method is less than R's value, whereas the R_{max}'s value is more significant than R's value when using the DS-PSO method. This comparison can be represented graphically, as in Figure 2.

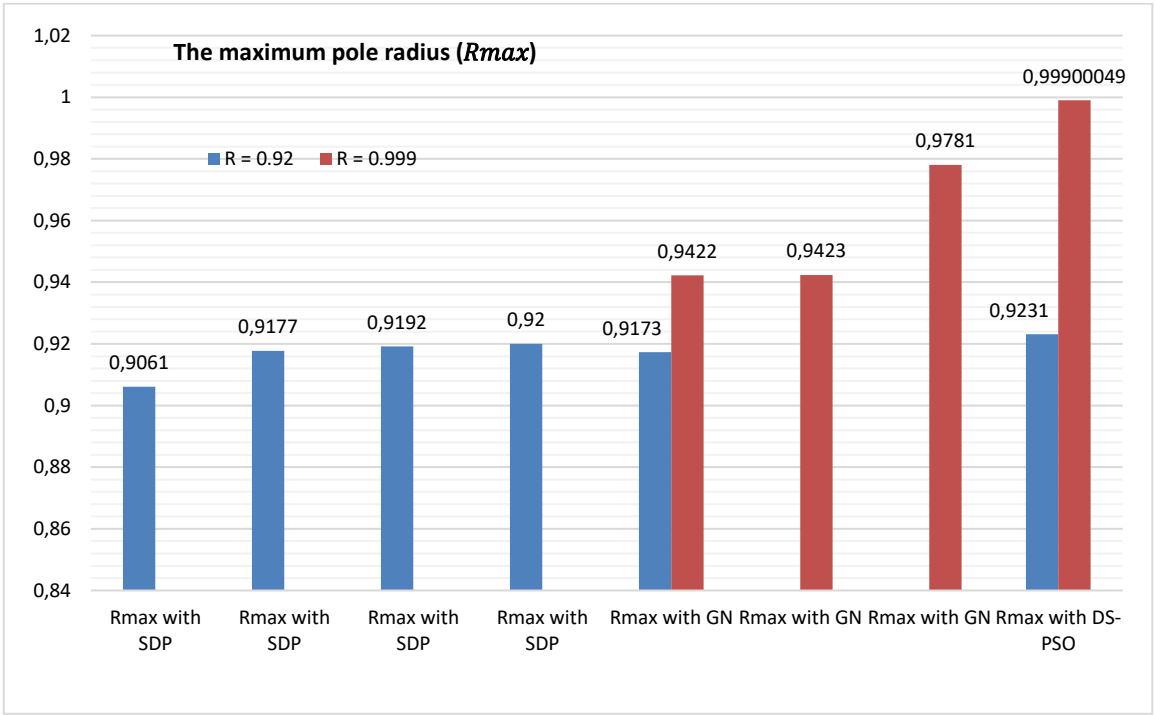

Figure 2. The graphical analysis for the values of maximum pole radius values **(**R_{max}).

Figure 2 is represented based on the data provided in Tables 3, 4, and 5 where an indicator of the R_{max} is shown in the top left of Figure 2, and the numbers on Figure 2's right side indicate the values of (R_{max}) that range (0.84 to 1.02). Likewise, the symbols or abbreviations (SDP, GN, and DS-PSO) on the lower side of the figure indicated the three methods used for comparison in this simulation.

It is clear that when R is equal to 0.92, the values' indicators of the R_{max} are different from one method to another, as in Figure 2, where the values' indicators of the R_{max} with SDP are lower than the values' indicators of the R_{max} with GN and (DS-PSO). The value's indicator of the (R_{max}) with GN is also lower than the value's indicator of the (R_{max}) with DS-PSO. In contrast, the value indicator of the (R_{max}) with DS-PSO higher than the values' indicators of the (R_{max}) with SDP and GN. Additionally, the value of the R_{max} indicator with (SDP

and GN) is not higher than 0.92. In contrast, the value of the R_{max} indicator with DS-PSO is higher than 0.92, where 0.92 is the predetermined value of R within the design parameters for the digital IIR elliptic filter; this value is mentioned in Table 2. Thus, this signifies that the R_{max} value achieved with the DS-PSO method surpasses both the predetermined R_{max} value and the maximum R_{max} values attained via GN and SDP.

Also, it is clear that when R is equal to 0.999, the values' indicators of the R_{max} are different from one method to another, as in Figure 2, where the value's indicator of the (R_{max}) with GN is lower than the value's indicator of the R_{max} with DS-PSO, and the value's indicator of the (R_{max}) with DS-PSO is higher than the values' indicators of the R_{max} with GN by the high rate, where 0.999 is the predetermined value of R within the design parameters for the digital IIR elliptic filter; this value is mentioned in Table 2. Thus, this signifies that the R_{max} value achieved with the DS-PSO method surpasses both the predetermined R_{max} value and the maximum R_{max} values attained via GN.

According to the experimental results obtained when designing a digital IIR elliptic filter with the parameters mentioned in Table 2. Additionally, the calculated value of (R_{max}) mentioned in the Tables (3, 4, and 5) and that obtained from the digital IIR elliptic filter design by utilizing the DS-PSO algorithm. We compared the values of the results the R_{max} by employing the DS-PSO algorithm that has been proposed and the values' results of the (R_{max}) with two methods from previous studies mentioned in the Tables (3, 4, and 5)**.**

Thus, graphical representation of the R_{max} values used for analysis by using the three different methods (SDP, GN, and DS-PSO) shown in Figure 2, it turned out that when R is equal to 0.92, the value of R_{max} close to 1.0 by a value ranging from 0.08 to 0.0939 when using SDP with 4th-order of the filter, As well as the value of R_{max} close to 1.0 by a value equivalent to 0.0827 when using GN with the fourth order of the filter, whereas the value of R_{max} close to 1.0 by a value equivalent to 0.0769 when using the DS-PSO algorithm with the fourth order of the filter.

Based on this, those values indicate that the R_{max} has the best value close to 1.0 when using the DS-PSO algorithm with the 4th-order for the develop of digital IIR filters. Because the (R_{max}'s) value is closest to 1.0; it is positioned inside the Z-plane unit circle, which resides in the plane, when using the DS-PSO algorithm with 4th-order for the digital IIR filter design**.**

On the other hand, it turned out that when R is equal to 0.999, the value of R_{max} is close to 1.0 by a value ranging from 0.0577 to 0.0578 when using GN with the fourth order of the filter and R_{max} is close to 1.0 by a value equivalent to 0.0219 when using GN with the 12th order of the filter. Whereas the value of R_{max} close to 1.0 by a value equivalent to 0.00099951 when using the DS-PSO with a filter's 4th-order and a filter's 12th-order. Thus, those values indicate that the R_{max} has the best value close to 1.0 when using the DS-PSO algorithm with fourth order and 12th order to develop a digital IIR filter. Because the R_{max} value is closest to 1.0; it is positioned inside the Z-plane unit circle, which resides in the plane, when using the DS-PSO algorithm with 4th order and 12th order to design digital IIR filters.

In case R is equal to 0.92, DS-PSO overcomes SDP with an average of 1.87% to 0.33%, and DS-PSO overcomes GN with an average of 0.63%. Therefore, the best value of R_{max} is obtained when DS-PSO is used to design the digital IIR elliptic filter, where the R_{max}'s value is 0.9231, greater by 0.0031 than the predefined R's.

Also, in case R is equal to 0.999, DS-PSO overcomes GN with an average of 6.0284% to 6.0172% when developing (elliptic) digital IIR filter of the fourth order, and DS-PSO overcomes GN with an average of 2.13% when developing (elliptic) digital IIR filter of the 12th order. Therefore, the best value of R_{max} is obtained when the develop (elliptic) digital IIR filter using DS-PSO with R is equal to 0.999, where the R_{max}'s value is equal to 0.99900049. This R_{max}'s value is greater than the predefined R's value.

These results are significant in solving the problems of the frequency response approximation with a desirable magnitude response for the digital IIR elliptic filter when the value of R is close to 1.0.

Table 6. Comparison Traditional Methods (SDP and GN) vs. Proposed Method (DS-PSO)

Parameter	SDP Method	GN Method	DS-PSO Algorithm	Difference (SDP vs. DS-PSO)	Difference (GN vs. DS-PSO)
Pole Radius (R)	0.92	0.92	0.92	-	-
Order of Filter	4th	4th	4th	-	-
R*max* (4th Order, R=0.92)	0.9061 - 0.92	0.9173	0.9231	**SDP < DS-PSO**	**GN < DS-PSO**
Pole Radius (R)	0.999	0.999	0.999	-	-
Order of Filter	4th	4th	4th	-	-
R*max* (4th Order, R=0.999)	-	0.9422 - 0.9423	0.99900049	**SDP < DS-PSO**	**GN < DS-PSO**
Pole Radius (R)	0.999	0.999	0.999	-	-
Order of Filter	12th	12th	12th	-	-
R*max* (12th Order, R=0.999)	-	0.9781	0.99900049	**SDP < DS-PSO**	**GN < DS-PSO**

Summary of Differences Traditional Methods (SDP and GN) vs. Proposed Method (DS-PSO) in Table 6:

- **SDP Method**: The R*max* values are consistently less than or equal to the predetermined R values for both 4th and 12th-order filters.
- **GN Method**: The R*max* values are consistently less than the predetermined R values for both 4th and 12th-order filters.
- **DS-PSO Algorithm**: The R*max* values are consistently greater than the predetermined R values for both 4th and 12th-order filters.
- The DS-PSO algorithm outperforms both the SDP and GN methods in terms of achieving higher R*max* values, which are closer to or exceed the predetermined R values. This indicates that the DS-PSO algorithm is more effective in designing digital IIR elliptic filters with higher pole radius values, especially for higher-order filters.

The purpose of this paper was realized when the optimal value of R_{max}, which was close to 1.0 when the DS-PSO algorithm was used to design of digital IIR elliptic filter, was determined. In this simulation, the value of R_{max} encouraged a large frequency response approximation with a desired magnitude response for the digital IIR elliptic filter. The main reason for obtaining this result is creating multiple topologies for each of the digital IIR elliptic filter's coefficients. In designing the digital IIR elliptic filter, employing dynamic and static topologies with PSO helped explore the search space and avoid preterm convergence; this led to solving the problem of the frequency response approximation with a desirable magnitude response for the digital IIR elliptic filter better than previously used methods (like SDP and GN). To verify this, see Figures 3, 4, and 5.

In Figures 3, 4, and 5, the circles (**o**) indicate the positions of zeros, and the crosses (×) indicate the position of poles. It is also evident that the number of crosses in Figures 3, 4, and 5 equals the designed filter's filter order number. Figures 3 and 4 show that the number of poles equals four because the 4th-order was applied in the digital IIR elliptic filter design. In contrast, in Fig. 5, the number of poles equals 12 because a digital IIR elliptic filter was designed using the 12th order. Similarly, the zeros' number equals the poles' number in Figures 3, 4, and 5; the number of poles is the same as the number of filter orders used to design an IIR elliptical filter**.**

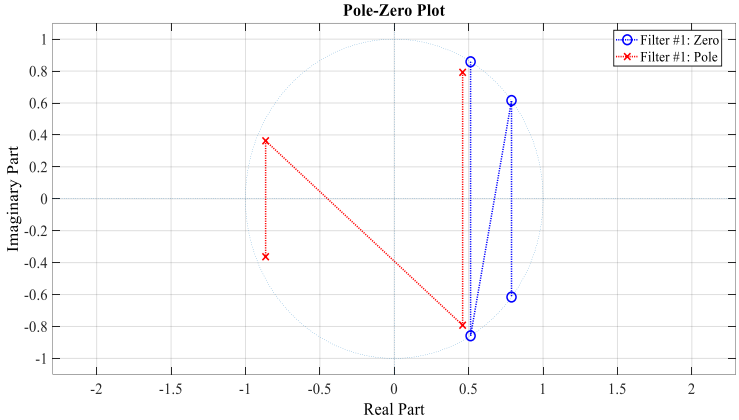

Figure 3. The pole-zero plot for the develop (elliptic) digital IIR filter with R= 0.92 and 4th order by DS-PSO.

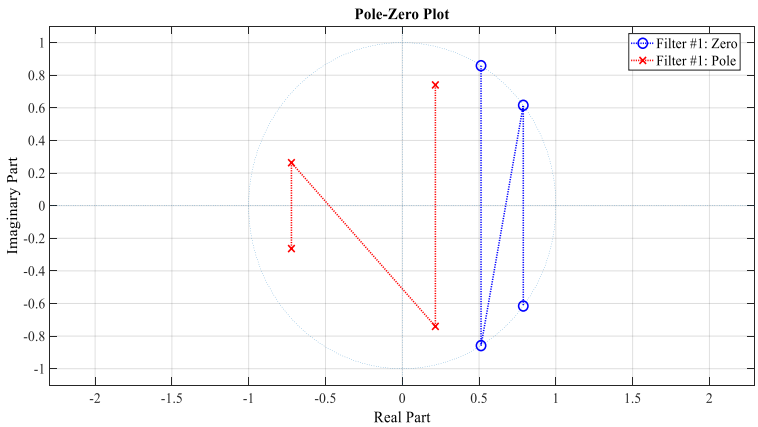

Figure 4. The pole-zero plot for the develop (elliptic) digital IIR filter with R= 0.999 and 4th order by DS-PS

The Pole-zero plot must be reviewed when presenting the digital IIR elliptic filter's design results to preview the poles' positions inside or outside the circle's unit. Additionally, the positions of the poles are among the essential things that must be paid attention to; this is to preview the stability condition of the filter during the digital filter design. However, the position of each pole must be previewed before calculating the value of R_{max} because the poles' positions relative to a unit circle represent the digital filter's stability condition. Therefore, the poles' positions relative to the unit circle were checked to check on the stability condition of the digital filter.

In case if any of the poles' positions are located outside the unit circle, the digital filter is unstable; in this case, the designed digital filter does not meet the stability condition. On the contrary, the digital filter has a stability condition when the unit circle contains all of the poles' positions; this stability condition has a different average than the value of R_{max}, depending on the method used to design the digital filter.

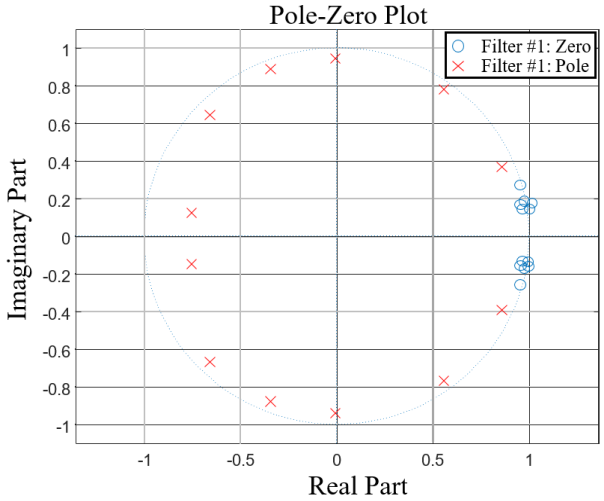

Figure 5. The pole-zero plot for a develop (elliptic) digital IIR filter with R= 0.999 and 12th order by DS-PS.

In Figures 3, 4, and 5 on the Z-plane, all poles' positions are inside the unit circle. Furthermore, the Z-plane appears to have a set of unique poles within the unit circle, as the poles' positions in Figures 3, 4, and 5 indicate that the (elliptic) digital IIR filter has the stability condition.

Finally, this paper fixes the problem of approximating the frequency response with a desirable digital IIR elliptic filter's magnitude response, and since this filter has the best value of R_{max} close to 1.0, the digital IIR elliptic filter was stable. Therefore, when using the DS-PSO algorithm, the digital IIR elliptic filter's stability is superior to that of prior methods, such as SDP or GN.

Table 7. Comparison Before and After Improvement.

Parameter	Before Improvement (SDP and GN)	After Improvement (DS-PSO)	Difference
Pole Radius (R)	0.92	0.92	-
Order of Filter	4th	4th	-
R_{max} (4th Order, R=0.92)	0.9061 - 0.92 (SDP) 0.9173 (GN)	0.9231	**SDP < DS-PSO** **GN < DS-PSO**
R_{max} Difference from 1.0	0.08 - 0.0939 (SDP) 0.0827 (GN)	0.0769	**SDP > DS-PSO** **GN > DS-PSO**
Pole Radius (R)	0.999	0.999	-
Order of Filter	4th	4th	-
R_{max} (4th Order, R=0.999)	0.9422 - 0.9423 (GN)	0.99900049	**GN < DS-PSO**
R_{max} Difference from 1.0	0.0577 - 0.0578 (GN)	0.00099951	**GN > DS-PSO**
Order of Filter	12th	12th	-
R_{max} (12th Order, R=0.999)	0.9781 (GN)	0.99900049	**GN < DS-PSO**
R_{max} Difference from 1.0	0.0219 (GN)	0.00099951	**GN > DS-PSO**
Average Improvement (R=0.92)	SDP: 1.87% - 0.33% GN: 0.63%	-	**SDP < DS-PSO** **GN < DS-PSO**
Average Improvement (R=0.999)	GN (4th Order): 6.0284% - 6.0172% GN (12th Order): 2.13%	-	**GN < DS-PSO**
Best R_max Value (R=0.92)	0.9231 (DS-PSO)	-	**SDP < DS-PSO** **GN < DS-PSO**
Best R_max Value (R=0.999)	0.99900049 (DS-PSO)	-	**GN < DS-PSO**

Summary of Comparison Before and After Improvement in Table 7:

- **Stability and Performance**: The DS-PSO algorithm significantly improves the stability and performance of digital IIR elliptic filters by achieving higher *R*max values closer to the predetermined R, especially for higher-order filters.
- **Efficiency and Accuracy**: The proposed DS-PSO algorithm outperforms traditional methods (SDP and GN) in terms of optimization efficiency and accuracy, providing more precise and stable filter designs.
- **Influence of Parameters**: The DS-PSO algorithm demonstrates that *R*max is primarily dependent on the predetermined R*R* and is not significantly affected by other design parameters, unlike traditional methods.
- **Best R*max* Values**: The DS-PSO algorithm consistently achieves the best *R*max values, which are closer to 1.0 within the Z-plane's unit circle, indicating superior filter stability and performance.
- The DS-PSO algorithm represents a substantial improvement over traditional methods for designing digital IIR elliptic filters. It ensures higher stability, greater efficiency, and more accurate filter designs, making it an optimal choice for practical applications in digital filter design.

6. CONCLUSION

Using the AI-based optimization approach called dynamic & static-particle swarm optimization (DS-PSO), the optimal design of a digital IIR elliptic lowpass filter was shown. Finding the optimal filter coefficients for the transfer function was the primary objective, and the DS-PSO technique and the ellip() function were used to achieve this. To ensure the stability of the suggested filter, it is crucial to accurately estimate the frequency response while maintaining an appropriate magnitude response. The significance of this became more apparent for R*max* values that were closer to one. Our simulation results show that the stability of the filter is R*max* dependent. This number is susceptible to the value of R but is unaffected by other design elements, such as the filter's setup or the values of the passband and stopband. According to earlier studies, each part of a filter design influences R*max*. However, the findings of this investigation reveal the exact reverse. The recommended DS-PSO approach makes getting the best results in any search field easy. Results for R*max* are comparable to or higher than the target R values when compared to more traditional methods like genetic algorithms (GA) and semi-definite programming (SDP). An excellent illustration of the DS-PSO algorithm's efficacy is its ability to produce filters of higher order. The DS-PSO method streamlines and simplifies the construction of digital IIR elliptic filters. This works well with fourth- and twelfth-order lowpass filters. Because it reliably yields higher R*max* values essential for filter stability it may be the optimal method to utilize with digital elliptic filters. This research provides engineers and academics with a reliable procedure for creating high-performance digital filters.

REFERENCES

[1] O. I. Omoifoi and T. Hinumoto, "Optimal design of stable recursive digital filters using unconstrained optimization methods," *2004 IEEE Asia-Pacific Conf. Circuits Syst.*, no. 1, pp. 517–520, 2004.

[2] B. Limketkai, W. Ng, and T. Rockwood, "Optimization-based synthesis of photonic iir filters accounting for internal losses in microresonators," *Journal of Lightwave Technology*, vol. 35, no. 20. pp. 4459–4467, 2017.

[3] X. Lai and Z. Lin, "Optimal design of constrained FIR filters without phase response specifications," *IEEE Transactions on Signal Processing*, vol. 62, no. 17. pp. 4532–4546, 2014.

[4] and Z. L. Lai, Xiaoping, Jiuwen Cao, "Minimax Magnitude Response Approximation of Pole-radius Constrained IIR Digital Filters.," *ICASSP 2019 - 2019 IEEE Int. Conf. Acoust. Speech Signal Process. (ICASSP).*, vol. 5, pp. 5491–5495, 2019.

[5] M. Kulkarni, J. K. S. Al-Safi, S. M. K. S. Reddy, S. B. G. T. Babu, P. Kumar, and P. Pushpa, "Early-Stage Timing Prediction in SoC Physical Design using Machine Learning," in *2023 International Conference on Artificial Intelligence and Knowledge Discovery in Concurrent Engineering (ICECONF)*, 2023, pp. 1–10.

[6] R. Parkavi, P. Karthikeyan, and A. S. Abdullah, "Enhancing personalized learning with explainable AI: A chaotic particle swarm optimization based decision support system," *Appl. Soft Comput.*, vol. 156, p. 111451, 2024.

[7] A. K. Roonizi, "Digital IIR filters: Effective in edge preservation?," *Signal Processing*, vol. 221, p. 109492, 2024.

[8] S. Chauhan, M. Singh, and A. K. Aggarwal, "Designing of optimal digital IIR filter in the multi-objective framework using an evolutionary algorithm," *Eng. Appl. Artif. Intell.*, vol. 119, p. 105803, 2023.

[9] J. Sun, J. Wang, Y. Wang, J. Li, and B. Cheng, "Improvement of IIR Digital Band-Pass Filter by the Digital Frequency Band Transformation," in *2023 IEEE 2nd International Conference on Electrical Engineering, Big Data and Algorithms (EEBDA)*, 2023, pp. 1187–1192.

[10] D. Izci and S. Ekinci, "Application of whale optimization algorithm to infinite impulse response system identification," in *Handbook of Whale Optimization Algorithm*, Elsevier, 2024, pp. 423–434.

[11] C. Lai and R. Zhao, "An Autocorrelation-Based r-Stability Condition With Application in the Design of IIR Filters," *IEEE Signal Process. Lett.*, 2024.

[12] K. Mallikarjunamallu and K. Syed, "Arrhythmia classification for non-experts using infinite impulse response (IIR)-filter-based machine learning and deep learning models of the electrocardiogram," *PeerJ Comput. Sci.*, vol. 10, p. e1774, 2024.

[13] B. Majhi, U. M. Mohapatra, and S. C. Satapathy, "Distributed machine learning strategies for efficient development of direct and inverse nonlinear and IIR models," *J. Ambient Intell. Humaniz. Comput.*, pp. 1–12, 2024.

[14] S. Ekinci and D. Izci, "Pattern search ameliorated arithmetic optimization algorithm for engineering optimization and infinite impulse response system identification," *Electrica*, vol. 24, pp. 119–130, 2024.

[15] Y. Dabas and N. Agrawal, "Improved Design and Optimization of IIR Filters by Cascading of ABC, PSO, and CA," in *Applications of Artificial Intelligence in Electrical Engineering*, IGI Global, 2020, pp. 332–343.

[16] F. Hammou and K. Hammouche, "An improved Particle Swarm optimization algorithm towards IIR system identification," *CCSSP 2020 - 1st International Conference on Communications, Control Systems and Signal Processing*. pp. 107–112, 2020.

[17] A. T. Alsahlanee, "Convergence Rate For Low-Pass Infinite Impulse Response Digital Filter," *J. Phys. Conf. Ser.*, vol. 1963, no. 1, p. 012103, Jul. 2021.

[18] A. T. Alsahlanee, "Digital Filter Performance Based on Squared Error," in *2021 International Conference on Advanced Computer Applications (ACA)*, 2021, pp. 74–79.

[19] D. Sanchez, "DS-PSO: Particle Swarm Optimization with Dynamic and Static Topologies," 2017.

[20] N. T. Gadawe, R. W. Hamad, and S. L. Qaddoori, "Realization of IIR Digital Filter Structures for ECG Denoising.," *J. Eur. des Systèmes Autom.*, vol. 57, no. 2, pp. 599–608, 2024.

[21] D. M. PERIŠIĆ, "NEW KIND OF IIR DIGITAL FILTERS INTENDED FOR PULSE PERIOD FILTERING," *Rev. Roum. DES Sci. Tech. ÉLECTROTECHNIQUE ÉNERGÉTIQUE*, vol. 69, no. 1, pp. 61–66, 2024.

[22] X. Tong, L. He, H. Du, and S. Dong, "A cascaded IIR filter with optimized group delay," *Proc. 14th IEEE Conf. Ind. Electron. Appl. ICIEA 2019*, no. 61674122, pp. 1990–1993, 2019.

[23] Y. Takase and K. Suyama, "A Diversification Strategy for IIR Filter Design Using PSO," in *2018 Asia-Pacific Signal and Information Processing Association Annual Summit and Conference (APSIPA ASC)*, 2018, pp. 1365–1369.

[24] B. Penumutchi and G. Tatikonda, "Systolic Digital IIR Filter Architectures for Real Time Signal Processing Applications," in *2024 5th International Conference for Emerging Technology (INCET)*, 2024, pp. 1–7.

[25] D. G. Lapitan, D. A. Rogatkin, E. A. Molchanova, and A. P. Tarasov, "Estimation of phase distortions of the photoplethysmographic signal in digital IIR filtering," *Sci. Rep.*, vol. 14, no. 1, p. 6546, 2024.

[26] K. O. Okpo and E. Omorogiuwa, "Optimizing Solar-Photovoltaic-Distributed Energy Resources in Power Networks using AI-based Particle Swarm Optimization (PSO) Algorithm."

[27] Q. Sun, X. Zhang, R. Jin, X. Zhang, and H. Zhang, "Multi-Strategy Equilibrium Optimizer Based on Comprehensive Improvement," in *Applied Mathematics, Modeling and Computer Simulation*, IOS Press, 2023, pp. 704–725.

[28] Q. Sun, X. Zhang, R. Jin, X. Zhang, and Y. Ma, "Multi-strategy synthetized equilibrium optimizer and application," *PeerJ Comput. Sci.*, vol. 10, p. e1760, 2024.